

AD-A115 741

CALIFORNIA UNIV BERKELEY ELECTRONICS RESEARCH LAB
PLASMA THEORY AND SIMULATION.(U)
MAR 81 C K BIRDSALL

F/G 20/9

UNCLASSIFIED

N00014-77-C-0578

NL

1 of 1
AC 3
10/74



END
DATE
FILMED
7 82
DTIC

AD A115741

DISTRIBUTION STATEMENT A

Approved for public release;
Distribution Unlimited

FIRST QUARTER PROGRESS REPORT on PLASMA THEORY AND SIMULATION

January 1 to March 31, 1981

Our research group uses both theory and simulation as tools in order to increase the understanding of instabilities, heating, transport, and other phenomena in plasmas. We also work on the improvement of simulation, both theoretically and practically.

Our staff is ----

<i>Professor C.K. Birdsall</i>	<i>191M</i>	<i>Cory Hall</i>	<i>(642-4015)</i>
<i>Principal Investigator</i>			
<i>Dr. Bruce Cohen,</i>	<i>L439</i>	<i>LLL</i>	<i>(422-9823)</i>
<i>Dr. William Nevins</i>	<i>L439</i>	<i>LLL</i>	<i>(422-7032)</i>
<i>Lecturers, UCB; Physicists LLL</i>			
<i>Dr. William Fawley</i>	<i>L321</i>	<i>LLL</i>	<i>(422-9272)</i>
<i>Dr. Alex Friedman</i>	<i>L477</i>	<i>LLL</i>	<i>(422-0827)</i>
<i>Guests, UCB; Physicists LLL</i>			
<i>Mrs. Yu-Jiuan Chen,</i>			
<i>Mr. Douglas Harned,</i>			
<i>Mr. Niels Otani,</i>			
<i>Mr. Stephane Rousset,</i>			
<i>Mr. Vincent Thomas</i>	<i>119MD</i>	<i>Cory Hall</i>	<i>(642-1297)</i>
<i>Research Assistants</i>			
<i>Mr. H. Stephen Au-Yeung</i>	<i>119ME</i>	<i>Cory Hall</i>	<i>(642-3477)</i>
<i>Programmer</i>			
<i>Ms. Ginger Pletcher</i>	<i>119ME</i>	<i>Cory Hall</i>	<i>(642-3477)</i>
<i>Secretary</i>			

March 31, 1981

DOE Contract DE-AT03-76ET53064-DE-AM03076SF00034

ONR Contract N00014-77-C-0578

ELECTRONICS RESEARCH LABORATORY

*University of California
Berkeley, California 94720*

**APPROVED FOR PUBLIC RELEASE
DISTRIBUTION UNLIMITED**

TABLE OF CONTENTS :

Section I

PLASMA THEORY AND SIMULATION

A.*	Lower Hybrid Drift Instability; 2d Simulations and Nonlocal Theory	page 3
B.	Velocity Space Aliasing	4
C.*	Hybrid Simulations of Theta Pinch Rotational Instabilities	10

Section II

CODE DEVELOPMENT AND MAINTENANCE

A.	Implicit Particle Simulation Using Moments with Orbit Averaging	11
B.	POLARES, A Two-Dimensional Electrostatic $R-\theta$ Code	15
C.	Plasma Sheath Simulation in 1d	15
D.	ICFT	16
E.	ES1 Code	17
F.	EM1 Code	17
G.	EZO HAR Code	17

Section III

SUMMARY OF REPORTS, TALKS, PUBLICATIONS, VISITORS

Distribution List	22
-------------------	----

* Indicates ONR supported areas

I. PLASMA THEORY AND SIMULATION

A. Lower Hybrid Drift Instability; 2d Simulations and Nonlocal Theory.

Yu-Jiuan Chen (Prof. C.K. Birdsall, W.M. Nevins, LLL)

The lower hybrid drift instability was studied with both a 2d electrostatic simulation code and a nonlocal theory. Results will be given in an ERL report now in preparation, to be submitted to the Physics of Fluids.

B. Velocity Space Aliasing.

Niels Otani, Dr. B.I. Cohen (LLL), and
Dr. M.J. Gerver (MIT) (Prof. C.K. Birdsall)

See contribution from LLL, following.



Accession For	
NTIS GRA&I	<input checked="" type="checkbox"/>
DTIC TAB	<input type="checkbox"/>
Unannounced	<input type="checkbox"/>
Justification	
By	
Distribution/	
Availability Codes	
Dist	Avail and/or Special
A	

Velocity-Space Aliasing Instability in Magnetized Quiet-Start Simulations

Bruce I. Cohen, William M. Nevins, and Neil Maron

Lawrence Livermore National Laboratory, University of California

Livermore, California 94550

In a continuing effort to develop a magnetized quiet-start simulation technique, we have studied analytically and in simulation the properties of distribution functions of velocities perpendicular to $B_0 \hat{z}$ composed of discrete speed classes (rings) and angle classes (spokes). A previous progress report¹ offered sufficiency conditions for stability of equally weighted rings and spokes Maxwellian distribution functions. Roughly speaking, if the number of velocity rings N_{v_\perp} satisfies $N_{v_\perp} > (1/3)(\omega_p/\omega_c)^2$ and the number of velocity spokes N_θ satisfies $N_\theta > 8(k_{\max} v_{th}/\omega_c)$, then stability of electrostatic flute modes ($\vec{k} \cdot \vec{B} = 0$) is expected ($v_{th} \equiv$ thermal velocity, $\omega_p \equiv$ plasma frequency, $\omega_c \equiv$ cyclotron frequency, $k_{\max} \equiv$ maximum wavenumber).

The stability of flute modes with respect to the number of velocity rings N_{v_\perp} and relative density ω_p^2/ω_c^2 was numerically determined by Kim and Otani neglecting the effects of discrete spokes.² Otani and Cohen¹ derived a dispersion relation including the coupling produced by discrete spokes,

$$\begin{aligned} \tilde{\phi}_r = \frac{4\pi n_0 q^2}{k^2} \int d\mu f_0(\mu) \left\{ \tilde{\phi}_r \sum_n \frac{n \partial J_n^2 / \partial \mu}{(\omega - r\omega_c) - n\omega_c} \right. \\ \left. + \sum_{n,m} \tilde{\phi}_{r-mN_\theta} \frac{[n \partial (J_n J_{n-mN_\theta}) / \partial \mu - m N_\theta J_{n-mN_\theta} \partial J_n / \partial \mu]}{(\omega - r\omega_c) - n\omega_c + m N_\theta \omega_c} \right\} \end{aligned} \quad (1)$$

where $\mu \equiv mv^2/2\omega_c$, $\phi(x,t) = \sum_r \tilde{\phi}_r \exp(ikx + i\omega_c t - i\omega t) + \text{c.c.}$,

and the Bessel functions have argument kv_\perp/ω_c . The effective frequency of mode $\tilde{\phi}_r$ is $\omega_r = \omega - r\omega_c$. Coupling to the spoke-induced cyclotron aliases will be negligible if the product $J_n J_{n-mN_\theta}$ is small.

The coupling of angular spokes deserves more discussion. For large index, the Bessel function is small in general and especially small for argument kv_\perp/ω_c less than the absolute value of the index. For argument much greater than the index, the magnitude of the Bessel function decreases as $(kv_\perp/\omega_c)^{-1/2}$; and the magnitude of the Bessel function is maximized for kv_\perp/ω_c comparable to the absolute value of the index. Possible couplings to cyclotron harmonics separated by $\pm N_\theta\omega_c$ ($m = \pm 1$) are the most likely to occur, if any alias coupling is going to occur at all. The arguments of the Bessel functions are naturally limited by the largest wavenumber and velocity

$$kv_\perp/\omega_c < 4k_{\text{max}}v_{\text{th}}/\omega_c \quad . \quad (2)$$

The product $J_n J_{n \pm N_\theta}$ will be small for all values of kv_\perp/ω_c if

$$4k_{\text{max}}v_{\text{th}}/\omega_c < \min \left[|n|, |n \pm N_\theta| \right] \leq N_\theta/2 \quad . \quad (3)$$

If Eq. (3) is not satisfied, cyclotron alias coupling can occur and instability may result. The first modes to couple as we increase the left side of Eq. (3) above the stability limit satisfy $|n| = |N_\theta \pm n| = N_\theta/2$; hence, $\omega_r \approx \pm N_\theta\omega/2$. A simulation example is pictured in Fig. 1. In this simulation, the parameters were $\omega_p^2/\omega_c^2 = 200$, $N_\theta = 32$, and $N_{v_\perp} = 299$. The distribution function was replicated eight times across the length of the system to quiet the first few spatial modes. The numerical solutions of Kim

and Otani² suggest that the distribution of rings should have been stable. For the mode pictured in Fig. 1, $kv_{th}/\omega_c = 6.25$ and velocities in the tail of the distribution $2.5 v_{th} \leq v_1 \leq 3 v_{th}$ give arguments falling near the maxima of J_ℓ , for $14 \lesssim |\ell| \lesssim 18$. Use of the ZED post-processor revealed the signature of the cyclotron alias coupling as lower hybrid normal modes near $\text{Re } \omega_r = \pm 14\omega_c$ coupled to modes at $\text{Re } \omega_r = \pm (14 - 32)\omega_c = \pm 18\omega_c$; these modes all grew with rate $\text{Im } \omega_r \approx 0.15 \omega_c$ and the ratios of the coupling modes were equal as expected, $|\phi(14\omega_c, k)|^2 / |\phi(-18\omega_c, k)|^2 = |\phi(-14\omega_c, k)|^2 / |\phi(18\omega_c, k)|^2$.

We doubled N_θ to $N_\theta = 64$, so that $4k_{\max}v_{th}/\omega_c = 25$, $N_\theta/2 = 32$, and Eq. (3) was satisfied. Figure 2 shows that modes near the lower hybrid frequencies $\text{Re } \omega_r = \pm 14\omega_c$ were excited and may have been very weakly unstable. However, if there was instability, saturation occurred very quickly and at a very small amplitude $E^2/8\pi nT = 10^{-11}$, which was not much above the initial amplitude. In fact, the fluctuation level in the normal modes was so small that the discrete particle ballistic noise was visible in the power spectrum (Fig. 2b). For our purposes, this simulation corresponded to a stable quiet start. We note in closing that Homer Meier explored some of these issues ten years ago.³

*This work was performed under the auspices of the U.S. Department of Energy at the Lawrence Livermore National Laboratory under contract W-7405-ENG-48.

1. N. F. Otani and B. I. Cohen, "An Electrostatic Dispersion Relation for a Uniform Magnetized Plasma Having a Discrete-Particle Velocity Distribution," Fourth Quarter Progress Report on Plasma Theory and Simulation, October 1 to December 31, 1980, Electronics Research Laboratory, U.C. Berkeley.

2. J. S. Kim and N. Otani, "Magnetized Multi-Ring Instabilities," Second Quarter Progress Report on Plasma Theory and Simulation, April 1 to June 30, 1980, Electronics Research Laboratory, U.C. Berkeley.
3. H. Meier, unpublished.

Figure Captions

Figure 1. Simulation of a Maxwellian plasma with a separable spokes and rings perpendicular velocity distribution function for electrostatic flute modes ($\vec{k} \cdot \vec{B} = 0$). The parameters were $\omega_p^2/\omega_c^2 = 200$, $kv_{th}/\omega_c = 1.25, 2.5, 3.75, 5$, and 6.25 , $N_{v_1} = 299$ and $N_\theta = 32$. (a) Perpendicular velocity distribution function. Apparent structure at low velocities is due to the particular sampling of 3000 particles out of the 76544 total. (b) Power spectrum $|\phi(\omega, k)|^2$ as a function of the frequency ω and (c) The corresponding field energy $E_k^2/8\pi$ integrated over ω as a function of time $\omega_c t$ for $kv_{th}/\omega_c = 6.25$.

Figure 2. Effectively stable spokes and rings simulation with the same plasma parameters as in Fig. 1 and with $N_{v_1} = 149$, $N_\theta = 64$ and 76288 total particles. (a) Sampling of perpendicular velocity distribution function. (b) Power spectrum $|\phi(\omega, k)|^2$ as a function of frequency ω and (c) $E_k^2/8\pi$ as a function of time $\omega_c t$ for $kv_{th}/\omega_c = 6.25$.

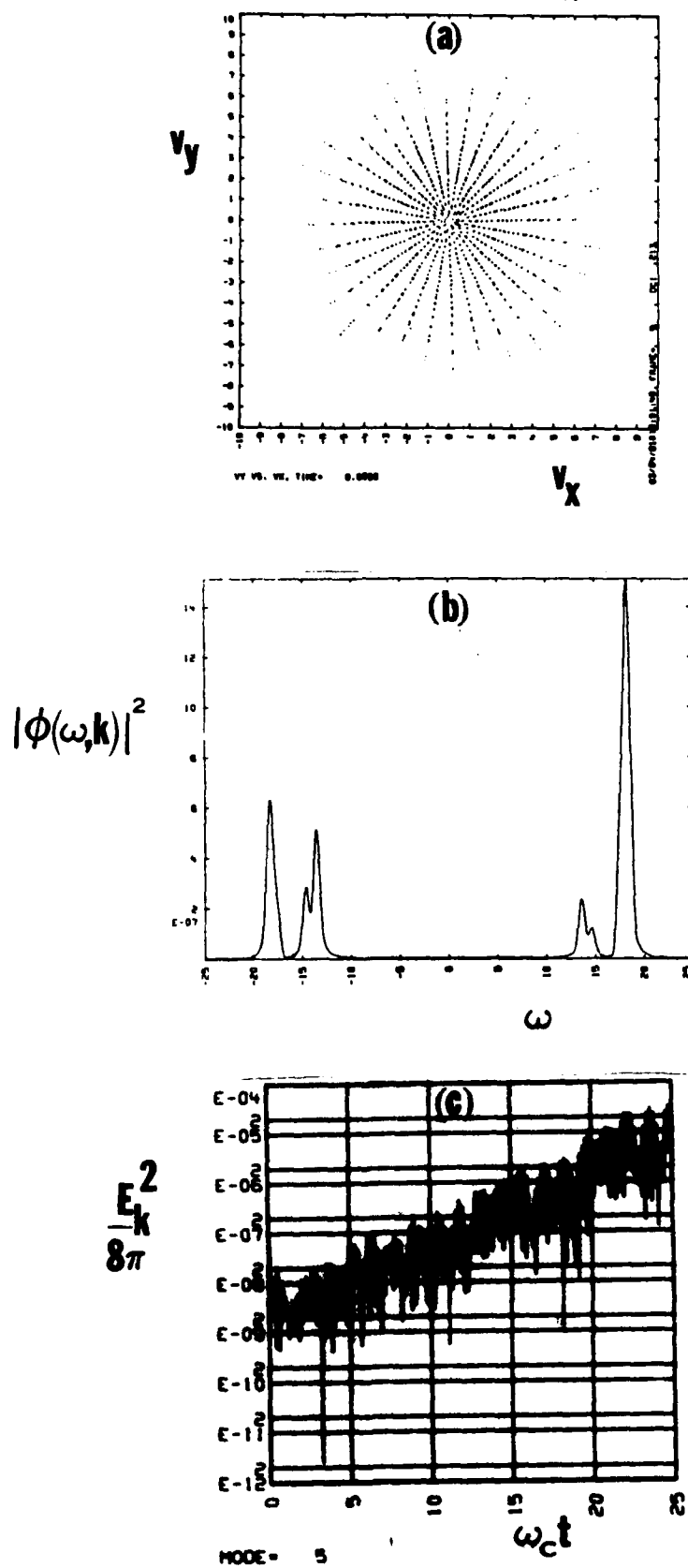


Figure 1

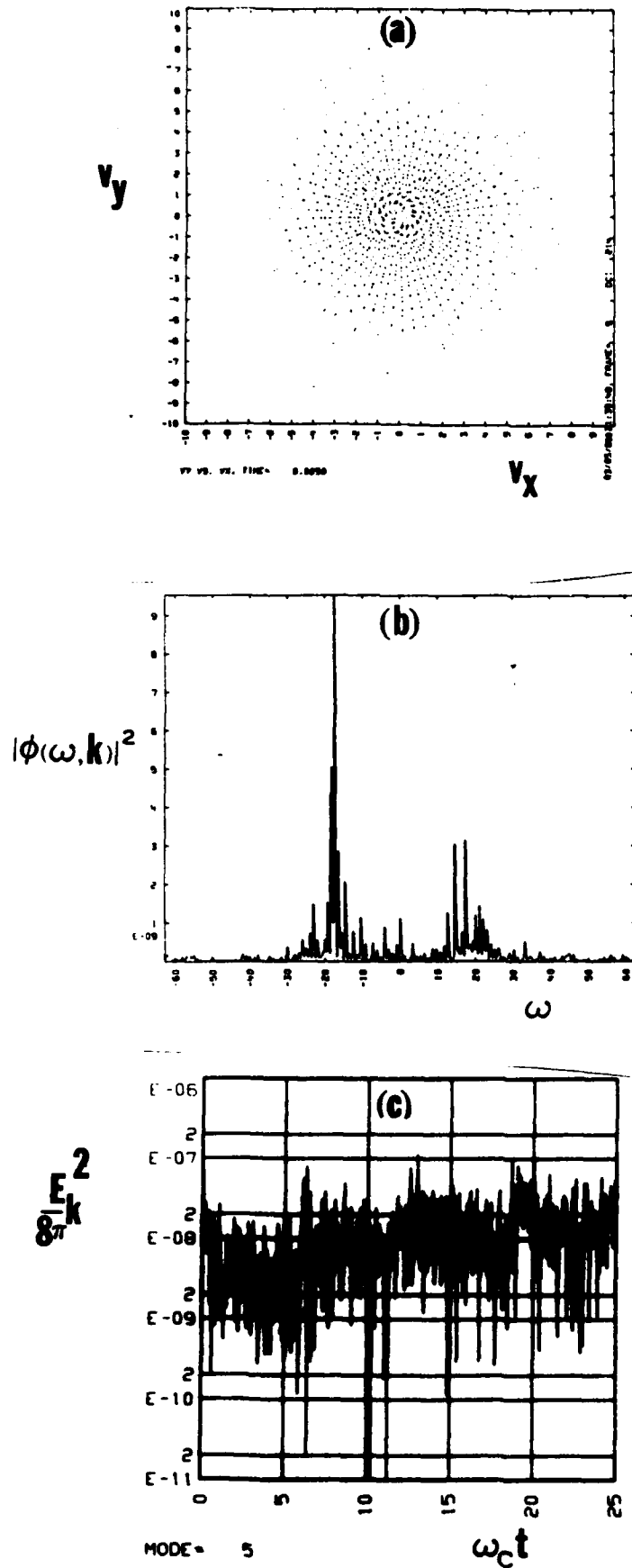


Figure 2

C. Hybrid Simulations of Theta Pinch Rotational Instabilities.

Douglas Harned (Prof. C. K. Birdsall)

Rotating rigid rotor theta pinch equilibria have been initialized in our two-dimensional hybrid code, AQUARIUS. The code now performs a three region solution of the field equations which properly treat the plasma-vacuum interface. Stationary equilibria have been found to be stable to all rotational instabilities, while equilibria with co-rotating ions and electrons have been found to develop an unstable $m=2$ mode. Growth rates have been measured and appear to be comparable to those predicted by the Vlasov-fluid theory of Seyler¹ and the finite Larmor radius theory of Freidberg and Pearlstein².

As the $m=2$ mode grows to large amplitude, nonlinear effects reduce the growth rate. This appears to be primarily due to stabilization by the conducting wall. However, the instability continues to grow at a reduced rate and leads to the eventual disruption of the plasma.

References

1. C.E. Seyler, "Vlasov-Fluid Stability of a Rigidly Rotating Theta Pinch," *Phys. Fluids* 22, 2324, (1979).
2. J.P. Freidberg, L.D. Pearlstein, "Rotational Instabilities in a Theta Pinch," *Phys. Fluids* 21, 1207, (1978).

II. CODE DEVELOPMENT AND MAINTENANCE

A. Implicit Particle Simulation using Moments with Orbit Averaging.

V. Thomas (Dr. B. I. Cohen LLL and Prof. C. K. Birdsall)

In our previous QPR we reported our initial failure to obtain a stable orbit averaged implicit moment code. We have since implemented many other algorithms in an attempt to create a stable code. One stable algorithm was found so far. We have developed model equations for our algorithms which correctly predict their stability for the case of linear cold plasma oscillations. Our stable orbit averaged code was used successfully to simulate a single mode ion acoustic wave. However, although we have constructed a stable orbit averaged implicit moment code, we apparently obtain no advantages over the non-orbit averaged implicit moment code as used by Mason for electrostatic wave propagation parallel to the magnetic field. The orbit averaged code is smaller but the number of operations cannot be reduced. We note in passing that for wave propagation parallel to the magnetic field a simple lag average of the pressure and current from previous time steps may prove effective in reducing the number of particles required for an implicit moment code. We have tried this in an implicit moment code and it is stable (except for a lag average of the density, which is apparently always unstable). Further study is needed to test for savings.

The stable orbit averaged algorithm employs particle ions and electrons to calculate the current density and the kinetic stress tensor on the simulation grid. The charge density is a fluid quantity and it is never accumulated from the particles in a direct fashion.

At a given time step N , the current density j is known at time step $N-1/2$, the kinetic stress tensor is known at time $N-1/2$, and the fluid density is known at time step N . The current density and the kinetic stress tensor are orbit averaged quantities and they are given by

$$j_s^{N-1/2} \equiv \frac{1}{(1 + \frac{\Delta T}{\Delta t_s})} \sum_{i=N\frac{\Delta T}{\Delta t_s}}^{i=(N+1)\frac{\Delta T}{\Delta t_s}} j_s^i \quad (1)$$

$$P_s^{N-1/2} \equiv \frac{1}{(1 + \frac{\Delta T}{\Delta t_s})} \sum_{i=N\frac{\Delta T}{\Delta t_s}}^{i=(N+1)\frac{\Delta T}{\Delta t_s}} P_s^i \quad (2)$$

Here s is the species label, ΔT is the field solve time interval, and Δt_s is the micro time step for species s .

The fluid density at time $N+1$ is obtained implicitly in terms of E^{N+1} through the use of

$$e_s n_s^{N+1} = e_s n_s^N - \frac{\partial}{\partial x} J_s^{N+1/2} \Delta T \quad (3)$$

$$J_s^{N+1/2} = j_s^{N-1/2} + \frac{e_s}{m_s} \left[e_s n_s^N E^* - \frac{\partial}{\partial x} P_s^{N-1/2} \right] \Delta T \quad (4)$$

Here E^* represents a linear combination of E^{N+1} , E^N , and E^{N-1} , J_s represents the fluid current density, and j_s represents the particle current density.

Next Poisson's equation is used to solve for the implicit field E^{N+1} as in

$$E^{N+1} = \int_0^x \sum_s e_s n_s^{N+1} dx + C \quad (5)$$

Here C is a constant to be determined from the boundary conditions. The particles are then advanced and the pressure term is recalculated. Equations (3) and (4) are used again to determine a new n_s^{N+1} and E^{N+1} . The particles are then re-advanced and the algorithm proceeds to

the next time step.

The model equations for the stable orbit averaging simulation method are given in the following four equations. The equations are valid for cold linear plasma oscillations in the limit of $k\Delta x \rightarrow 0$.

$$ikE^{N+1} = e\delta n^{N+1} \quad (6)$$

$$e(\delta n^{N+1} - \delta n^N) = -ikJ^{N+1/2}\Delta T \quad (7)$$

$$J^{N+1/2} = j^{N-1/2} + e^2 \frac{n_0}{m} \Delta TE^* = e \frac{n_0}{2} (v^{N-1} + v^N) + e^2 \frac{n_0}{m} \Delta TE^* \quad (8)$$

$$v^{N+1} = v^N + \frac{e}{m} \Delta TE^* \quad (9)$$

$$E^* = \alpha E^{N+1} + \beta E^N + (1 - \alpha - \beta) E^{N-1} \quad (10)$$

The dispersion relation we obtain is

$$-(z-1)^2 = \omega_p^2 \Delta T^2 \left[z + \frac{1}{2z} - \frac{1}{2} \right] \left[\alpha z + \beta + \frac{(1-\alpha-\beta)}{z} \right] \quad (11)$$

Here $z = e^{-i\omega\Delta T}$ and α and β are parameters.

Two test runs were made for the stable algorithm. The amplification factors obtained from the dispersion relation agreed with those obtained by simulation to three places. For $\omega_p \Delta T = 0.2$ the simulation value for the amplification factor was 0.990 whereas for the dispersion relation we expect the value 0.990. For $\omega_p \Delta T = 4$, the simulation value for the amplification factor was 0.727 versus the value predicted by the dispersion relation of 0.728. Comparison of the model equations with 3 unstable schemes gave results almost as good as these. All simulations were performed using infinitely massive ions and cold electrons with excitations of approximately 10^{-4} of a particle separation distance.

One concern for the stable algorithm is the possible divergence of the fluid density with the particle density, since the fluid density is never accumulated from the particles. To test this over a long time scale we performed a single mode ion acoustic simulation to the time $24000 \omega_p^{-1}$. The fluid charge density and the particle charge density accumulated from the grid are shown in Figure 1 and in Figure 2 respectively. The results appear to be satisfactory. The plot of the ion kinetic energy vs. time in Figure 3 exhibits the correct frequency. The theoretical damping rate is not easily seen from the plot. The field energy for this run is shown in Figure 4.

For the ion acoustic runs that used E^* equal to E^{N+1} , the algorithm was unstable for $k_{\max} v_{te} \Delta T \geq 0.1$ in contrast to the method employed by Mason where there is no such stability limit when a fully implicit field corresponding to our E^{N+1} is used. With further modification of the orbit averaging algorithm it might be possible to relax the $k_{\max} v_{te} \Delta T$ constraint.

We have simulated a single mode ion acoustic wave using Mason's method to compare with our orbit averaged simulation. Figure 5 shows the ion kinetic energy for the simulation and Figure 6 shows the field energy.

We chose the number of particles for this simulation so that the orbit averaged simulation and this simulation would have the same number of particle pushes (i.e. so that both simulations would require a similar number of computer operations, ignoring for the moment the fact that the orbit averaged code has a predictor and a corrector step and no corrector step was used for our Mason's method simulation). From Figures 3 to 6 it is clear that orbit averaging has not helped to eliminate noise and furthermore, resonant particle effects appear to be better represented by our Mason's method simulation. The ion kinetic energy from our Mason's method simulation shows damping throughout the entire simulation from $t = 0$ to $t = 24000 \omega_p^{-1}$, although the damping is slower than the Landau rate. This may be due to finite grid effects. In contrast there is no damping in the orbit averaged code. In fact the ion

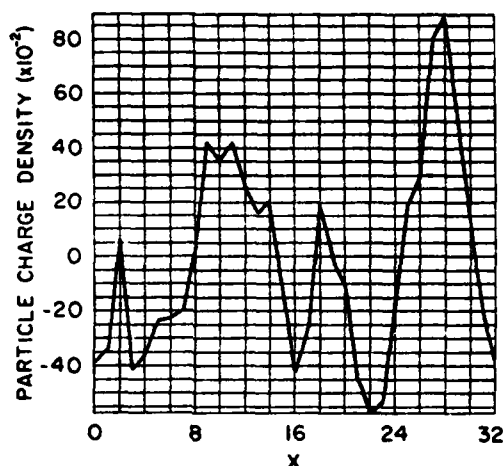


Figure 1. The particle charge density averaged over a macrostep at time $t = 20800\omega_p^{-1}$. For this simulation we have used: $m_i/m_e = 25$, $\omega_{pe}\Delta T = 4$, $\Delta t_i = \Delta t_e = 0.2$, $v_{te} = 0.025$, $v_{ti} = 0.0$, $NG = 32$, $\Delta x = 1$, $Np = 512$, $E^* = E^{N+1}$, and the ions were given an initial sinusoidal velocity perturbation in the simulation mode (mode 1) with amplitude $v_1 = -0.0005$. The fluid density was initialized in a self consistent manner.

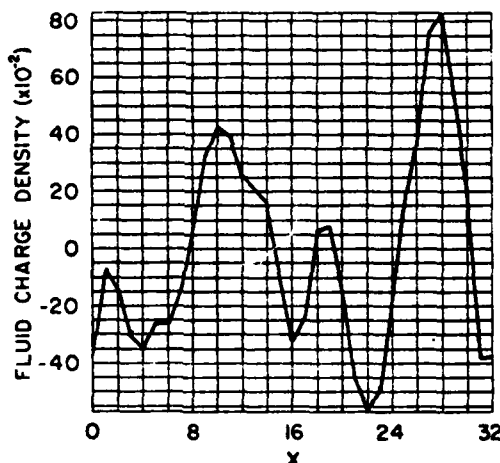


Figure 2. The fluid charge density at time $t = 20800\omega_p^{-1}$.

kinetic energy reaches a maximum of approximately 50% larger than the initial excitation at the end of the orbit averaged simulation. Also the noise in the field energy is greater for the orbit averaged simulation than for the Masons' method simulation. This is due to the fact that the particles are not able to fill in much of phase space during a macrostep because of the very restrictive condition on $k_{max} v_{te} \Delta T$.

Orbit averaging cannot improve particle statistics over the implicit moment particle simulation method in the unmagnetized electrostatic limit because the moment implicit method uses a field solve time step that is the same as the desired particle time step; i.e., the largest ΔT that still accurately resolves the particle orbit. The source term for the orbit average electric field contains $(\Delta T/\Delta t)NP1$ input variables, where $NP1$ is the number of particles. The source term for the implicit moment simulation method contains $NP2$ input variables. In order to achieve the same statistical behavior in the two sources we might expect to require the same number of particle pushes, $(\Delta T/\Delta t)NP1 = NP2$, in which case averaging would not give savings, even for the same ΔT . The situation with this orbit averaged code is, in fact, worse than this because one may use a larger ΔT with the implicit moment method and still retain stability (although

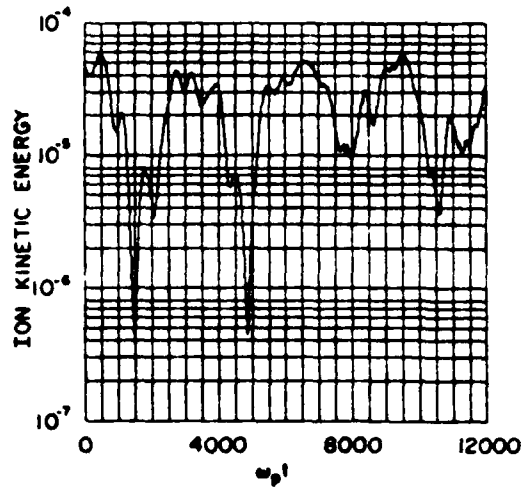


Figure 3. The ion kinetic "sloshing" energy from $t = 0$ to $t = 12000\omega_p^{-1}$.

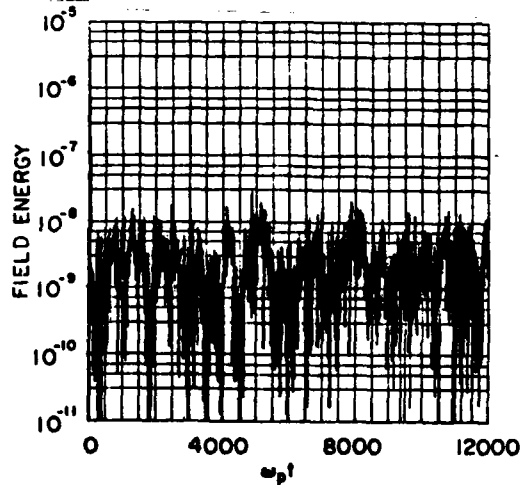


Figure 4. The electrostatic energy from $t = 0$ to $t = 12000\omega_p^{-1}$.

we still require $k_{\max} v_{te} \Delta T \ll 1$ to retain all of the physics).

These results are in contrast to the results obtained when orbit averaging was used in a magneto-inductive code.* In that instance the number of particles required for the simulation was dramatically reduced due to the fact that ΔT was made very large. Also, since the particles were moved with $\Omega_c \Delta t \ll 1$ the cyclotron motion was treated accurately.

For cases where one needs to accurately treat wave phenomena parallel to a magnetic field or in its absence, one needs $k_{\max} v_{te} \Delta T \ll 1$. If this is the most severe constraint on ΔT for accurate particle motion, it is impossible for orbit averaging to give any great advantage if one can move the particles in time steps of ΔT with the use of another method. For cases where $\Omega_c \Delta T \gg 1$, orbit averaging gives more accurate gyromotion.

It is important to note that these remarks are true when the wave has a component along the field lines. For the other case orbit averaging can offer advantages.** The reader is referred to that paper for

*Cohen B. I., Brengle T. A., Conley D. B., and Freis R. P., "An Orbit Averaged Particle Code," *J. Comput. Phys.* 38, 45, Nov. 1980.

**Freis R. P., Cohen B. I., Byers J. A., and Thomas V. A., "Orbit Averaged and Implicit Particle Codes", Annual Sherwood Controlled Fusion Theory Conference, paper IC11 Univ. of Texas, Austin, Texas, April 1981.

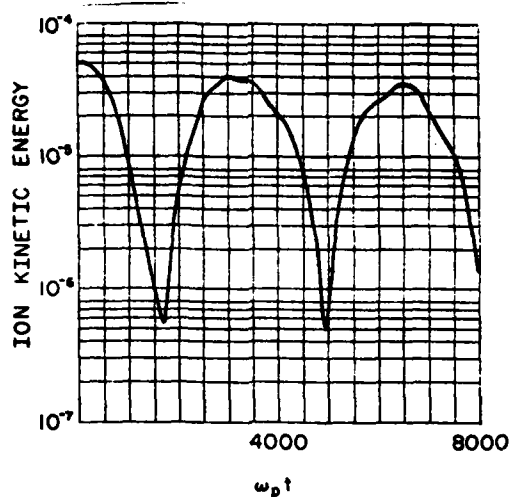


Figure 5. The ion kinetic "sloshing" energy from $t = 0$ to $t = 8000\omega_p^{-1}$. Here, $N_p = 10240$ and the other parameters are the same as for the orbit averaged simulation.

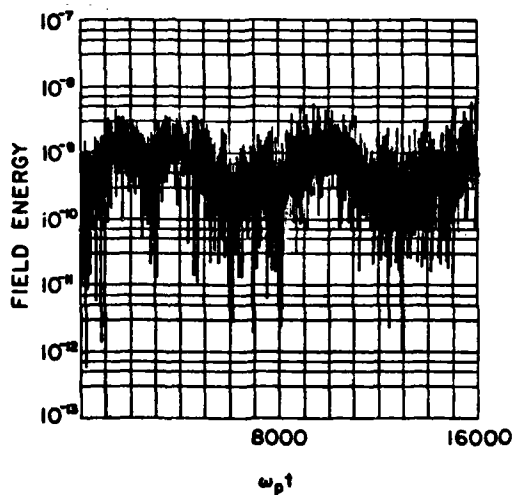


Figure 6. The electrostatic energy from $t = 0$ to $t = 8000\omega_p^{-1}$.

that case.

B. POLARES.

Niels F. Otani (C. K. Birdsall)

No special progress to report.

C. PLASMA SHEATH SIMULATION IN 1d.

S. Rousset (Prof. C. K. Birdsall)

Modifications to the ES1 code have been written so as to allow the simulation of a plasma sheath. In the model used, we have a plasma reservoir in the half-space $x \leq 0$ and a metal

target at $x=L$. Depending on the externally applied potential between $x=0$ and $x=L$, on the external magnetic field and on the initial velocity, a particle can or cannot reach the target. The purpose of this study is to describe the velocity distribution on the target, the current density, instabilities, etc.

In order to have a periodic numerical model to describe this nonperiodic physical model, we first compute the true charge density in the $0 < x < L$ region, and we add an inverted charge density in the $L < x < 2L$ region so that $\rho(L+x) = -\rho(L-x)$. This is the same as considering that for each charge in the true sheath, there is an image charge (opposite sign) in the inverted sheath.

Note that only the charge density and the fields are computed in the inverted region; there is actually no particle outside the true region: the equations of motion are integrated in the $0 < x < L$ region only, and whenever the mover brings a particle from a point within the sheath to a point $x < 0$ or $x > L$, the particle disappears.

At present the code is in its preliminary testing stages. No major problem has yet been encountered.

References

- C. K. Birdsall, W. B. Bridges, *Electron Dynamics of Diode Regions*, Academic Press, 1966.
- I. Langmuir, "The Effect of Space Charge and Initial Velocities on the Potential Distribution and Thermoionic Current Between Parallel Electrodes," *Phys. Rev. Lett.* 21, 419, 1921.
- I. Langmuir, H. Mott-Smith, *Gen. Elec. Rev.* 27, 449, 1924.

D. ICFT.

H. Stephen Au-Yeung

ICFT is a preprocessor of CFT. It allows the user to specify include files within the source program.

An include file contains a sequence of Fortran statements. For those who are familiar with the CHATR compiler on the CDC-7600, an include file has similar functions to a cliché (see the CHATR manual). To refer to an include file, the user puts the include statement in one of the two following formats:

- (1) Within a comment statement -

```
c include FileName
```
- (2) Not within a comment statement -

```
include FileName
```

When ICFT reaches an include statement, it opens the specified file and replaces the statement by whatever is in the file. After replacing all the include statements, ICFT then invokes CFT to perform the compilation.

ICFT resides in the FILEM directory .CRAY of user number 1222. To obtain ICFT from the CRAY-1 computer, the user may type:

```
FILEM READ 1222 .CRAY ICFT(ESC)END
```

An example may make this document clearer:

The following is a main program contained in the file - SOURCE.

```
c An example to show how to use the include file.
c
c      include identify
c
parameter ( CPW=8, BPW=64 )
parameter ( NS=10 )
```

```

integer Line(10)
c
include initial
c
call msgtor ( "Example of include file", 23 )
call exit
end

```

The file IDENTIFY contains

```

c AUTHOR:      H. Stephen Au-Yeung
c INSTITUTION: University of California, Berkeley

```

and the file INITIAL contains

```

call dropfile ( 0 )
call msglink ( 59, 1 )

```

The input on the execution line of ICFT is the same as that of CFT plus an optional ILIB entry. A typical example is:

```
ICFT I=SOURCE,B=BINARY,L=0,ILIB=(ICFT,INCLUDE)
```

where ICFT and INCLUDE are both LIB files. If an include file is not found under the active file index, ICFT opens the libraries specified in the ILIB entry, ICFT and INCLUDE in this case, and looks for the file. If there needs only one include library, the parentheses can be omitted. When no ILIB entry is given, only the active file index is searched.

Notes:

- (1) Include statements may also appear within include files. The nesting can go as deep as 10.
- (2) Each include library may contains at most 200 entries.

E. EM1 Code.

No special progress to report.

F. ES1 Code.

No special progress to report.

G. EZOHAR Code.

No special progress to report.

III. SUMMARY OF REPORTS, TALKS, PUBLICATIONS, VISITORS

Journal publication:

Nevins, W.M., Y. Matsuda, and M.J. Gerver, "Plasma Simulations Using Inversion Symmetry as a Boundary Condition," *J. Comput. Phys.* 39, 1, January 1981.

Abstracts of 3 talks submitted to conferences follow.

Submitted to Sherwood Theory Meeting, Austin Texas
April 8-10, 1981

Lower Hybrid Drift Instability; Theory and 2d Simulations

Yu-Jiuan Chen and C. K. Birdsall
Electronics Research Laboratory
University of California
Berkeley, CA 94720

William M. Nevins
Lawrence Livermore National Laboratory
University of California
Livermore, CA 94550

The lower hybrid drift instability is being studied with both a 2-d electrostatic simulation code and a nonlocal theory. A slab configuration is used with a density gradient in x . In the initial equilibrium, the ion pressure gradient cancels the zeroth order ambipolar electric force. Since the characteristic frequency of the lower hybrid drift instability is much greater than the ion cyclotron frequency, the ions are treated as unmagnetized particles.

Simulations show good agreement of the measured growth rate and frequency with the results of local theory during the early stage of wave growth. At later times nonlocal effects become important, and a coherent mode structure develops. This normal mode is observed to propagate up the density gradient. The mean wave vector is $\underline{k} = k_x \hat{x} + k_y \hat{y}$, in good agreement with our nonlocal theory.

At zero plasma beta and zero electron temperature, we found that the lower hybrid drift instability is stabilized by the local current relaxation occurring in two separate regions. The neighborhood of the point where the electrons have the greatest relative drift velocity is the most unstable region according to local theory. In this region the current relaxes by modification of the ion velocity distribution. However, in our nonlocal theory, the wave propagates into the plasma to a second region where the electron drift velocity equals the phase velocity of the most unstable wave. In this second region the electrons are in resonance with the wave and local current relaxation occurs by modification of the electron density profile.

* This research was supported in part by the Office of Naval Research under Contract N00014-77-C-0578 (Berkeley), and in part by the Department of Energy under Contract No. W-7405-ENG-48 (Livermore).

Submitted for poster session, Sherwood Theory Meeting, Annual Controlled Fusion Theory Conference, Austin, Texas, April 8-10, 1981.

Submitted to Sherwood Theory Meeting, Austin, Texas, April 8-10, 1981

ROTATIONAL INSTABILITIES IN FIELD-REVERSED CONFIGURATIONS;

RESULTS OF TWO-DIMENSIONAL HYBRID SIMULATIONS

Douglas S. Harned

Electronics Research Laboratory
University of California, Berkeley

Rotational instabilities in field-reversed configurations are being studied using a two-dimensional hybrid simulation code. The code treats ions as particles and electrons as an inertialess fluid. Fields are described by the Darwin version of Maxwell's equations (i.e., the transverse displacement current is neglected) and the electron momentum equation, coupled by the assumption of quasineutrality. Ions are moved by the equations of motion. Linear weighting is used to determine forces, densities, and ion currents. The code has been applied to two configurations: (1) a tenuous high-current ion layer immersed in a dense background plasma, and (2) a field-reversed theta-pinch.

In field-reversed ion layers instabilities may arise due to a coupling of layer betatron oscillations with compressional Alfvén waves in the background plasma. The hybrid simulations, as well as a numerical extension of previous theoretical work, have demonstrated that instabilities may occur in thin layers at levels of field-reversal below those previously predicted. This result implies that field-reversed ion layers must be very thick to be stable. The simulations show that instability growth causes heating within the layer, which results in the layer expanding, reducing the betatron frequency. The shift in betatron frequency prevents the resonant interaction of particles with the compressional Alfvén waves, ending instability growth. After all instability growth has stopped the layer is still field-reversed, but much thicker. The final state appears to be relatively stable and is characterized by large electron currents and many non-axis-encircling ions.

The field-reversed theta-pinch has been simulated to study rotational instabilities driven by centrifugal forces. Unstable $m=2$ modes have been observed when the magnitude of the ion rotational frequency exceeds that of the difference between the ion and electron rotational frequencies, as expected. Preliminary results indicate linear growth rates comparable to those predicted by finite Larmor radius MHD and Vlasov-fluid models.

Work supported by ONR Contract No. N00014-17-C0578

Poster session requested

Sherwood Fusion Theory Conf., Austin, Texas, April 8-10, 1981

ORBIT-AVERAGED AND IMPLICIT PARTICLE CODES

R. P. Freis, B. I. Cohen, and J. A. Byers
Lawrence Livermore National Laboratory, University of California
Livermore, California 94550
and V. A. Thomas, University of California at Berkeley
Berkeley, California 94720

ABSTRACT

Significant progress has recently been made in extending the applicability of particle codes to long time scale plasma phenomena. This has been accomplished by means of orbit-averaging and implicit techniques that relax the usual time step constraints required for numerical stability of conventional explicit differencing schemes. The important features of the orbit-averaged implicit methods are substantial reduction of particles, unconditional stability of the field equation(s) solution at large time step, and tailoring and splitting of particle time scales by species and even by velocity class to accurately and efficiently resolve particle trajectories. Some of the more important applications we anticipate are two-dimensional and limited three-dimensional kinetic simulations of equilibrium formation and transport in tandem mirrors with thermal barriers and gun-produced field-reversed mirrors and of low frequency drift waves or MHD instabilities with finite Larmor radius effects naturally included. The new simulation techniques allow use of much more realistic simulation parameters.

We report the successful implementation of new implicit methods and merging of orbit averaging¹ with the moment equation field implicit method independently developed by Mason² and Denavit³ and with the direct implicit particle method due to Langdon, Friedman and Cohen. We have analytically determined rudimentary stability and filtering characteristics and confirmed stable code operation with a linearized electrostatic code and nonlinear one-dimensional electrostatic and two-dimensional magneto-inductive codes. Orbit averaging by itself may lead to numerical instability depending on the underlying physics model. Merging orbit averaging with one of the implicit methods may not give a stable or convergent scheme unless sufficient implicitness is preserved. We will exhibit code results on the simulation of ion acoustic waves and the multiple time-scale simulation of mirror machine build-up, equilibrium and transport.

We have also developed a particular form of the Mason implicit technique² in a linearized particle code that accurately reproduces growth rates and real frequencies for ion cyclotron instabilities and low frequency gravity-driven interchange modes with FLR stabilization effects properly calculated. This code allows any value of $\omega_{pe}\Delta t \gg 1$.

1. B. I. Cohen, T. A. Brengle, D. B. Conley, and R. P. Freis, J. Comp. Phys. 38, 45 (1980).
2. R. J. Mason, "Moment Equation Field Implicit Particle Simulation of Plasmas," Los Alamos Scientific Laboratory Report LA-UR-80-2171, August 1, 1980.
3. J. Denavit, "Time Filtering Particle Simulations with $\omega_{pe}\Delta t \gg 1$," Lawrence Livermore National Laboratory Report UCRL-85097, October 1980.

*This work was supported by the U.S. Department of Energy under Contract No. W-7405-ENG-48 at Lawrence Livermore National Laboratory and DOE Contract AS03-76SF00034-DE-AT03-76ET53064 at U.C. Berkeley.

POSTER SESSION

DISTRIBUTION LISTDepartment of Energy

Manley, Nelson, Sadowsky, Drobott
Lankford

Department of Navy

Condell, Roberson, Florance

Austin Research Associates

Drummond, Moore

Bell Telephone Laboratories

Hasegawa

Calif. Institute of Technology

Liewer

Calif. State Polytech. Univ.

Rathman

Columbia University

Chu

Cornell University

Mankofsky

Electrical Power Research Inst.

Gough, Scott

General Atomic Company

Helton, Lee

Hascom Air Force Base

Rubin

JAYCOR

Klein, Tumolillo, Hobbs

Kirtland Air Force Base

Pettus

Los Alamos Scientific Laboratory

Barnes, Forslund, Gitomer, Hewett, Lindemuth,
Mason, Neilson, Oliphant, Sgro

Lawrence Berkeley Laboratory

Cooper, Kaufman, Kim, Kunkel, Pyle,
Sternlieb

Lawrence Livermore National Laboratory

Albritton, Anderson, Brengle, Briggs,
Bruijnes, Byers, Chambers, Cohen, Drupke,
Estabrook, Fawley, Finan, Fries, Fuss, Harte,
Killeen, Kruer, Langdon, Lasinski, Lee,
Maron, Matsuda, Max, McNamara, Mirin, Nevins,
Nielson, Smith, Tull, Friedman

Mass. Institute of Technology

Berman, Bers, Gerver, Kulp, Palevsky

Mission Research Corporation

Godfrey

U. S. Naval Research Laboratory

Boris, Drobot, Craig, Haber, Orens,
Vomvoridis, Winsor

Northwestern University

Crystal, Denavit

New York University

Grad, Weitzner

Oak Ridge National Laboratory

Dory, Meier, Mook

Princeton Plasma Physics Laboratory

Chen, Cheng, Lee, Okuda, Tang

Princeton University

Graydon

DISTRIBUTION LISTScience Applications, Inc.

McBride, Siambis, Wagner

Sandia Laboratories, Albuquerque

Freeman, Poukey, Quintenz, Humphries

Sandia Laboratories, Livermore

Marx

Massachusetts

Johnston

Stanford University

Buneman

University of Arizona

Morse

University of California, BerkeleyArons, Au Yeung, Birdsall, Chen,
Chorin, Grisham, Harned, Hudson,
Keith, Lichtenberg, Lieberman,
McKee, Otani, Potter, ThomasUniversity of California, Davis

DeGroot, Woo

University of California, Irvine

Rynn

University of Calif., Los Angeles

Dawson, Decky, Huff, Lin

University of Iowa

Joyce, Knorr, Nicholson

University of Maryland

Guillory, Rowland, Winske

University of Pittsburgh

Zabusky

University of Texas

Horton, McMahon, Tajima

University of Wisconsin

Shohet

Culham Laboratory

Eastwood, Roberts

University of Reading

Hockney

Ecole Polytechnique/Centre de Physique Theorique

Adam

Bhabha Atomic Research Centre

Aiyer, Gioel

Isreal

Gell

Tel-Aviv University

Cuperman

Kyoto University

Abe

Nagoya University

Kamimura

Max Planck Institut fur Plasmaphysik

Biskamp, Kraft

Universitat Kaiserslautern

Wick

University of Innsbruck

Kuhn